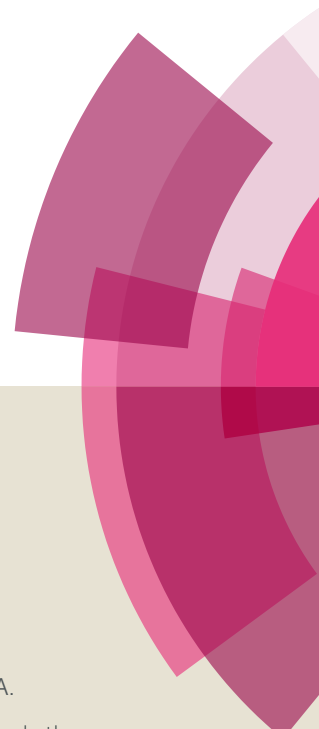


MedChemComm

Accepted Manuscript



This article can be cited before page numbers have been issued, to do this please use: D. Zhang, D. Tong, D. Yang, J. Sun, F. Zhang and G. Zhao, *Med. Chem. Commun.*, 2018, DOI: 10.1039/C8MD00197A.



This is an Accepted Manuscript, which has been through the Royal Society of Chemistry peer review process and has been accepted for publication.

Accepted Manuscripts are published online shortly after acceptance, before technical editing, formatting and proof reading. Using this free service, authors can make their results available to the community, in citable form, before we publish the edited article. We will replace this Accepted Manuscript with the edited and formatted Advance Article as soon as it is available.

You can find more information about Accepted Manuscripts in the [author guidelines](#).

Please note that technical editing may introduce minor changes to the text and/or graphics, which may alter content. The journal's standard [Terms & Conditions](#) and the ethical guidelines, outlined in our [author and reviewer resource centre](#), still apply. In no event shall the Royal Society of Chemistry be held responsible for any errors or omissions in this Accepted Manuscript or any consequences arising from the use of any information it contains.

Design, synthesis and biological evaluation of AKT inhibitors bearing a piperidin-4-yl appendant

Daoguang Zhang^{1,†}, Dongdong Tong^{2,†}, Dezhi Yang³, Jing Sun⁴, Fenghe Zhang^{2,*}, Guisen Zhao^{1,*}

¹Department of Medicinal Chemistry, Key Laboratory of Chemical Biology (Ministry of Education), School of Pharmaceutical Sciences, Shandong University, Jinan, Shandong 250012, PR China

²Department of Oral and Maxillofacial Surgery, School of Stomatology, Shandong University, Shandong Provincial Key Laboratory of Oral Tissue Regeneration, Jinan, Shandong 250012, PR China

³National Pharmaceutical Experimental Teaching Demonstration Center, School of Pharmacy, Zunyi Medical University, Zunyi, Guizhou 563003, PR China

⁴Department of Bone Metabolism, School of Stomatology, Shandong University, Shandong Provincial Key Laboratory of Oral Tissue Regeneration, Jinan, Shandong 250012, PR China

[†]These authors contributed equally to this work.

*Corresponding author:

Fenghe Zhang: Department of Oral and Maxillofacial Surgery, Shandong Provincial Key Laboratory of Oral Tissue Regeneration, School of Stomatology Shandong University, Jinan, Shandong 250012, PR China. Tel & Fax: +86-531-88382961. E-mail: zfengh@sdu.edu.cn

Guisen Zhao: Department of Medicinal Chemistry, Key Laboratory of Chemical Biology (Ministry of Education), School of Pharmaceutical Sciences, Shandong University, Jinan, Shandong 250012, PR China. Tel & Fax: +86-531-88382009. E-mail: guisenzhao@sdu.edu.cn

Abstract

A series of AKT inhibitors possessing a piperidin-4-yl side chain was designed and synthesized. Some of them showed high AKT1 inhibitory activity and potent

anti-proliferative effect on PC-3 prostate cancer cells in the preliminary screening. Further studies revealed the most potent compound, **10h**, as a pan-AKT inhibitor. Compound **10h** was able to inhibit the cellular phosphorylation of AKT effectively and induce apoptosis of PC-3 cells. It also showed high metabolic stability in human liver microsomes. As a promising lead AKT inhibitor, preclinical characterization of **10h** as a potential anti-prostate cancer therapeutic needs to be further investigated.

1. Introduction

Hyperactive aberration of PI3K-AKT signaling is observed in a wide variety of cancer types, which makes components of this signaling possible targets for cancer therapy¹. The serine/threonine kinase AKT, also known as protein kinase B (PKB), plays a critical role in this signaling and is hyper-activated in over 50% of human tumors². It regulates by phosphorylation over one hundred downstream substrates that are involved in the regulation of various cellular events, including cell survival, proliferation and metabolism. Glycogen synthase kinase 3 (GSK3) is the first reported substrate of AKT³, and evaluation of the phosphorylation level of its β isoform is typically used as a tool assessing the intracellular inhibition level of AKT by small molecule inhibitors.

Given that AKT is tightly linked to cell physiology and pathology, it has been catching attention of the pharmaceutical world in the past decades. A number of AKT-targeted agents have entered clinical trials for an exploration of their therapeutic potential against various tumor types. For instance, **AZD5363** (Figure 1) was investigated for its safety and efficacy in prostate cancer in a phase 1 clinical trial (NCT01692262). Particularly, since activation of the PI3K-AKT signaling through loss of the tumor suppressor PTEN was proven as a potential mechanism for the pathology of castration-resistant prostate cancer (CRPC)⁴, AKT inhibitors have been utilized in combination therapy for the treatment of CRPC, such as a phase 2 trial of **AZD5363** in combination with enzalutamide in metastatic CRPC (NCT02525068).

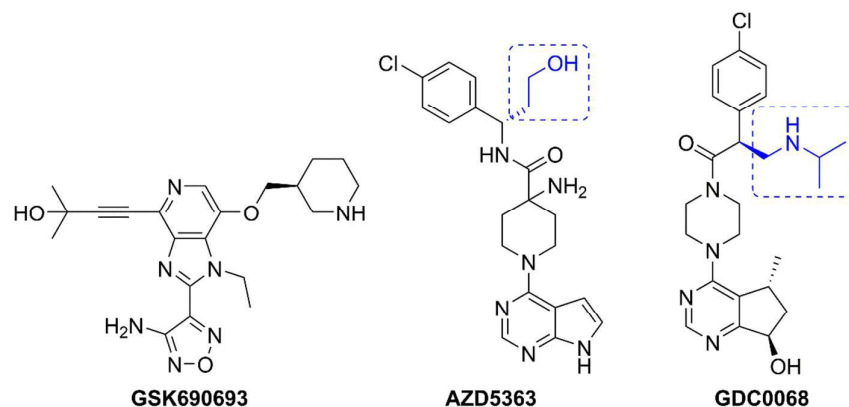


Figure 1. ATP-competitive inhibitors of AKT in clinical trials

Among all the AKT inhibitors reported, a specific type of ATP-competitive inhibitors, including **GSK690693**, **AZD5363** and **GDC0068**, was well developed (Figure 1)⁵. Analysis of the co-crystals of **AZD5363**⁶ or **GDC0068**⁷ in complex with AKT revealed that these agents bond to the hinge region of AKT. The modes of this ligand-protein interaction can be capitalized in the discovery of novel AKT inhibitors.

Our laboratory previously reported a series of AKT inhibitors with general structure shown in figure 2⁸. Represent compounds **5q** and **5t** in this series showed high AKT1 inhibition at the concentration of 50 nM with inhibitory rates of 69.7% and 65.5%, respectively. Both compounds also exhibited moderate anti-proliferative effect in a prostate cancer cell line of PC-3 with IC₅₀ values of 21.1 μM and 31.5 μM, respectively. In this work, structural modification was further performed. First, since the hydrogen bond interactions, formed between the hydroxyethyl group of **AZD5363** or isopropylaminomethyl group of **GDC0068** and the carboxyl residues of two glutamic acids (Glu 234 and Glu 278) near the hinge region, were critical for their ligand-protein binding affinity^{6,7}. So, one modification to our lead structure was to introduce an appendant to the bridging methylene between the carbonyl and phenyl groups (Figure 2). The criteria for this appendant was that it should provide a hydrogen bond donor to generate similar hydrogen bond interactions without introduction of chirality. After a literature survey, a piperidin-4-yl group which had been adopted by previously reported AKT inhibitors **AI-1** (AKT IC₅₀ = 18 nM) and **AI-2** (AKT IC₅₀ = 20 nM) was adopted (Figure 2)^{9,10}. This was a symmetric cyclic

appendant with a terminal imine group as the hydrogen bond donor. The other modification focused on the hinge-binding pyrrolopyrimidine group, three nitrogen-containing bicyclic systems were attempted in this work. These modifications led to a series of *N*-heterocyclic based AKT inhibitors.

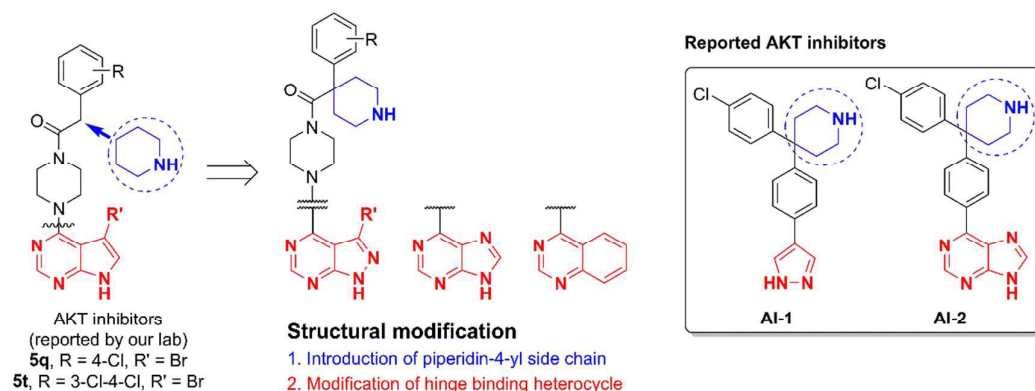


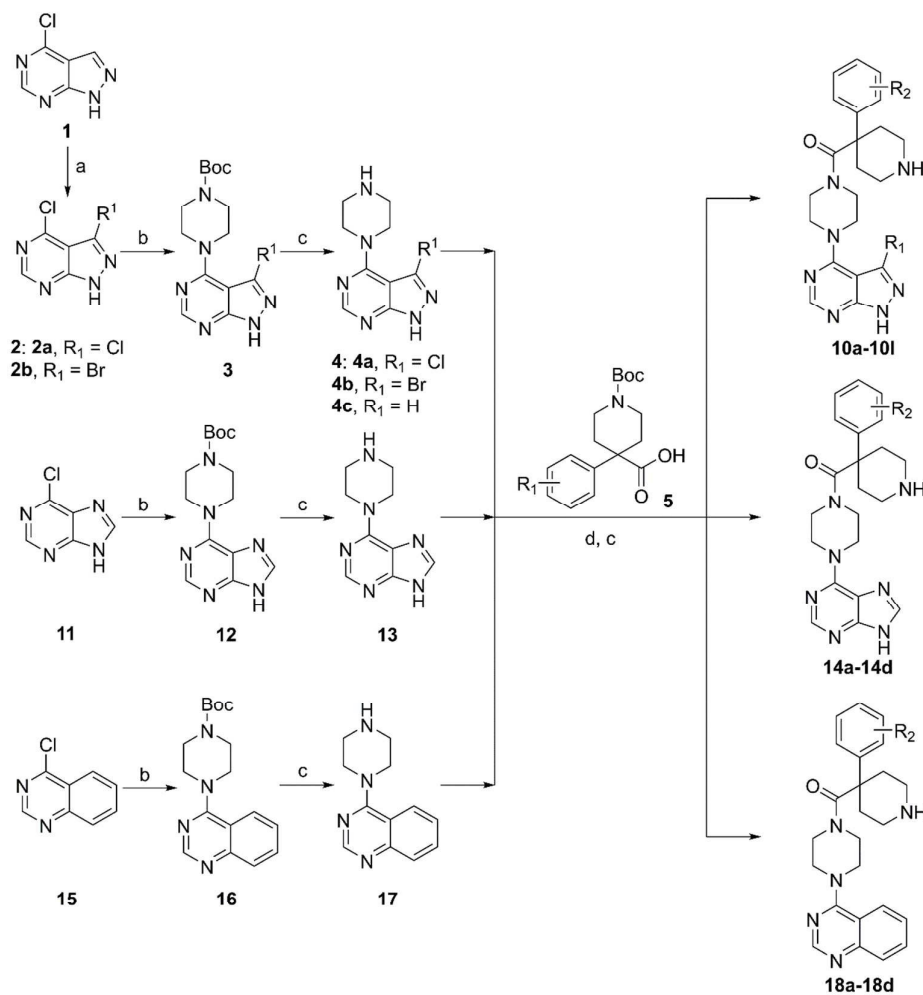
Figure 2. Design of novel ATK inhibitors based on our and others' previous studies

2. Results and discussion

2.1. Chemistry

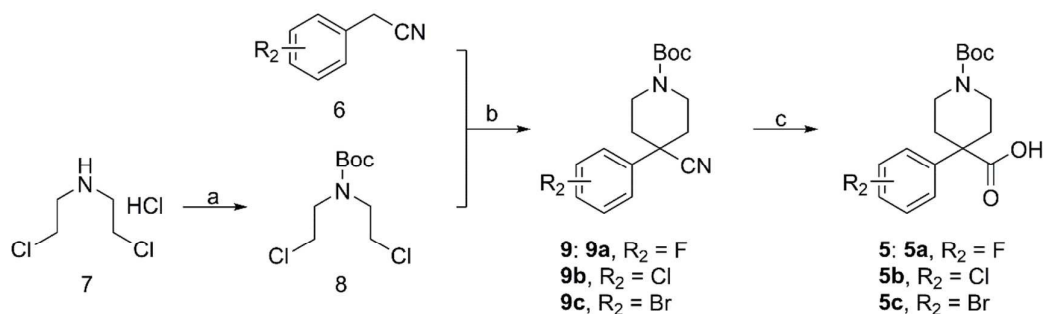
Compounds **10a-10l** were prepared following the route as shown in scheme 1. Halogen groups like chloride or bromide were first introduced at C-5 position of a commercially available 4-chloropyrazolopyrimidine (**1**) via a free radical halogenation. Aromatic nucleophilic substitution of the chloride from C-4 position of intermediate **2** by *tert*-butyl piperazine-1-carboxylate under microwave irradiation afforded intermediate **3**, which was de-protected with trifluoroacetic acid (TFA) to give intermediate **4**. Finally, condensation with a proper carboxylic acid (**5**) followed by de-protection of the Boc protective group afforded compounds **10a-10l**.

This synthetic route was successfully applied to the preparation of compounds **14a-14d** and **18a-18d** using 6-chloro-9*H*-purine (**11**) and 4-chloroquinazoline (**15**) as starting materials, respectively (Scheme 1).



Scheme 1. Reagents and conditions: (a) NCS or NBS, DMF, r.t., 12-18 h; (b) *tert*-butyl piperazine-1-carboxylate, DMF, microwave, 150 °C, 20 min; (c) TFA, DCM, r.t., 4 h; (d) HBTU, DIPEA, DMF, r.t., 6 h; (e) TFA, DCM, r.t., 4 h.

4-chlorobenzylcyanide (**6**) was used as a starting material for the preparation of building block **5** (Scheme 2). The two hydrogen atoms of the methylene group of **6** were first abstracted by sodium hydride, followed by replacing of the two chlorine atoms from Boc-protected bis(2-chloroethyl)amine (**8**) to afford the substituted 4-phenylpiperidine-4-carbonitrile as intermediates **9**. A subsequent hydrolysis generated the carboxylic acid as intermediate **5**.



Scheme 2. Reagents and conditions: (a) aq. NaOH, (Boc)₂O, DCM, r.t., 12 h; (b) NaH, DMF, 0-5 °C; 80 °C, 12-18 h; (c) NaOH, ethanol, 60 °C, 48 h.

2.2. AKT inhibitory activity and anti-proliferative effect on PC-3 cells

Preliminary screenings were carried out for the newly synthesized compounds, including the evaluation of AKT inhibitory activity at a compound concentration of 1 μM and of anti-proliferative effect on a Prostate cancer cell line of PC-3 (Table 1).

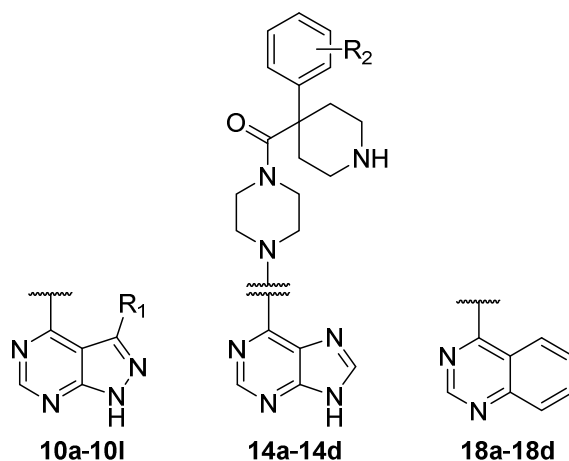
Compounds (**14a-14d**) containing a purine ring exhibited higher AKT1 inhibitory activity than their pyrazolopyrimidine analogues (**10a-10d**) and quinazoline analogues (**18a-18d**), but lacked anti-proliferative activity. Compounds (**18a-18d**) bearing a quinazoline structure showed low AKT1 inhibition but high anti-proliferation, while pyrazolopyrimidine-derived compounds (**10a-10d**) lacked both AKT1 inhibitory activity and cytotoxicity. However, introduction of a halogen substituent to the C-3 position of the pyrazolopyrimidine ring significantly elevated inhibitory activity against both AKT1 and PC-3 cells. Compounds (**10e-10l**) with a halogen substitution (Cl or Br) at the C-3 position of the pyrazolopyrimidine ring exhibited both high AKT inhibition and high growth inhibition in PC-3 cells than did their hydrogen substituted counterparts (**10a-10d**).

For compounds (**10a-10l**) based on a pyrazolopyrimidine ring with or without halogen substituent on C-3 position, substitutions on the terminal phenyl ring had different influences. All of the 4-F substituted compounds (**10a**, **10e** and **10i**) showed weaker AKT1 inhibition at 1 μM than their chlorine or bromine substituted analogues. This tendency was confirmed at a diluted concentration of 0.1 μM as compounds (**10e** and **10l**) showed inferior AKT1 inhibition than their chlorine or bromine substituted analogues **10f-10h** and **10j-10l**. Similar trend was also observed on the potency

against PC-3 cells, as compounds (**10f-10h** and **10j-10l**) with chlorine or bromine substitution all showed higher anti-proliferative activity than their 4-F substituted analogues (**10e** and **10i**).

Based on the preliminary data on both AKT1 inhibition and PC-3 cell growth inhibition, compounds (**10f-10h** and **10j-10l**) were selected for the determination of AKT1 inhibitory IC_{50} values (Table 1). In comparison with the positive drug **GSK690693**, these compounds all showed slightly lower AKT1 inhibitory activity. Among them, compound **10h** showed the highest AKT1 inhibitory activity with an IC_{50} value of 24.3 nM, and was most potent against PC-3 cells with an IC_{50} value of 3.7 μ M. This cellular potency was nearly 4-fold more effective than **GSK690693** (IC_{50} = 14.1 μ M).

Table 1. Preliminary screenings for the new compounds: AKT1 inhibition and anti-proliferation in PC-3 cells.



Code	Structure		AKT1 inhibition			Anti-proliferative effect on PC-3 cells (IC_{50}/μ M) ^b
	R ₁	R ₂	%, @1 μ M ^a	%, @0.1 μ M ^a	IC_{50}/nM ^b	
10a	H	4-F	7.4	-	-	> 40
10b	H	4-Cl	38.7	-	-	> 40
10c	H	4-Br	11.6	-	-	> 40
10d	H	3,4-diCl	52.1	-	-	> 40
10e	Cl	4-F	86.7	60.9	-	37.4 \pm 2.2
10f	Cl	4-Cl	91.9	83.4	66.6 \pm 2.1	19.4 \pm 1.6
10g	Cl	4-Br	95.4	84.5	32.9 \pm 1.9	32.4 \pm 2.1
10h	Cl	3,4-diCl	94.3	83.7	24.3 \pm 1.6	3.7 \pm 0.9

10i	Br	4-F	93.2	53.3	-	36.6 ± 2.4
10j	Br	4-Cl	96.7	86.7	26.9 ± 1.7	9.8 ± 1.2
10k	Br	4-Br	96.5	90.6	51.9 ± 2.1	15.0 ± 1.3
10l	Br	3,4-diCl	93.8	90.9	30.5 ± 1.8	10.3 ± 1.1
14a	-	4-F	94.2	-	-	> 40
14b	-	4-Cl	45.6	-	-	> 40
14c	-	4-Br	68.0	-	-	> 40
14d	-	3,4-diCl	51.4	-	-	33.9 ± 2.2
18a	-	4-F	23.0	-	-	13.7 ± 1.3
18b	-	4-Cl	34.2	-	-	> 40
18c	-	4-Br	6.1	-	-	22.8 ± 1.6
18d	-	3,4-diCl	21.9	-	-	14.0 ± 1.8
GSK690693			99.5	98.5	21.3 ± 2.1	14.1 ± 1.6

^an = 3

^bIC₅₀ data are mean of three independent experiments

2.3. Kinase selectivity study of selected compound 10h

Compound **10h** was further evaluated for its selectivity against a panel of 16 kinases (Figure 3) at the concentration of 1 μM. This compound showed high AKT1 selectivity over 11 kinases (Abl, B-Raf, CDK1, CHK1, GSK3β, JAK1, PDK1, PKCα, RAF-1 and ROCK1). However, compound **10h** showed moderate inhibitory activity against MNK1 (47%) and Aurora A (64%), and high inhibitory activity against RSK1 (83%), PKA (99%) and p70S6K (99%). The lack of selectivity against the latter three kinases was mainly due to high overall ATP binding site homology (>70%) of these kinases with AKT1¹¹.

At the concentration of 10 nM, compound **10h** showed pan-inhibitory activity to all three AKT isoforms with moderate to high inhibition of AKT2, AKT1 and AKT3 by 38%, 83% and 93%, respectively (Figure 3). A more than 2-fold selectivity of AKT1 and 3 against AKT2 was also observed.

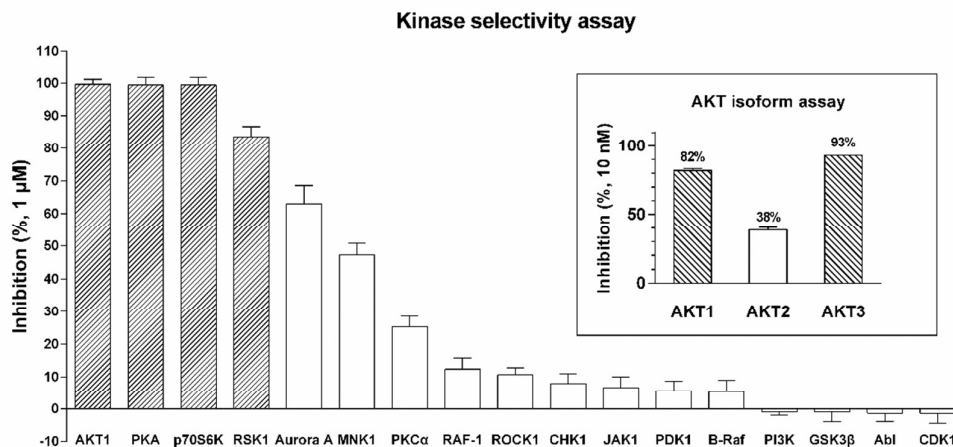


Figure 3. Selectivity assay for **10h** in 16 human kinases and three AKT kinase isoforms (n = 3).

2.4. Influence of **10h** on cellular AKT and GSK3 β phosphorylation

Compound **10h** was further evaluated for its impact on cellular AKT signaling in PC-3 cells *via* an immunoblotting assay (Figure 4A). Contrary to **GSK690693** which enhanced AKT activation in this assay, a high inhibition of AKT phosphorylation by **10h** was observed after 24 hours of treatment at all three concentrations. Similar phenomenon also occurred on reported AKT inhibitors based on a diphenylmethanamine scaffold¹², and indicated an involvement of additional functional mechanism for compound **10h** to overcome the positive feedback loop which usually was evoked to fight back the AKT inhibition within the cells. In the meantime, **10h** showed weaker inhibition on the phosphorylation of GSK3 β , a downstream effector of AKT, compared with efficient inhibition of GSK3 β phosphorylation by **GSK690693**. This was consistent with the distinct function of the two compounds on AKT phosphorylation as GSK3 β was directly downstream and suppressed by activated AKT within cells.

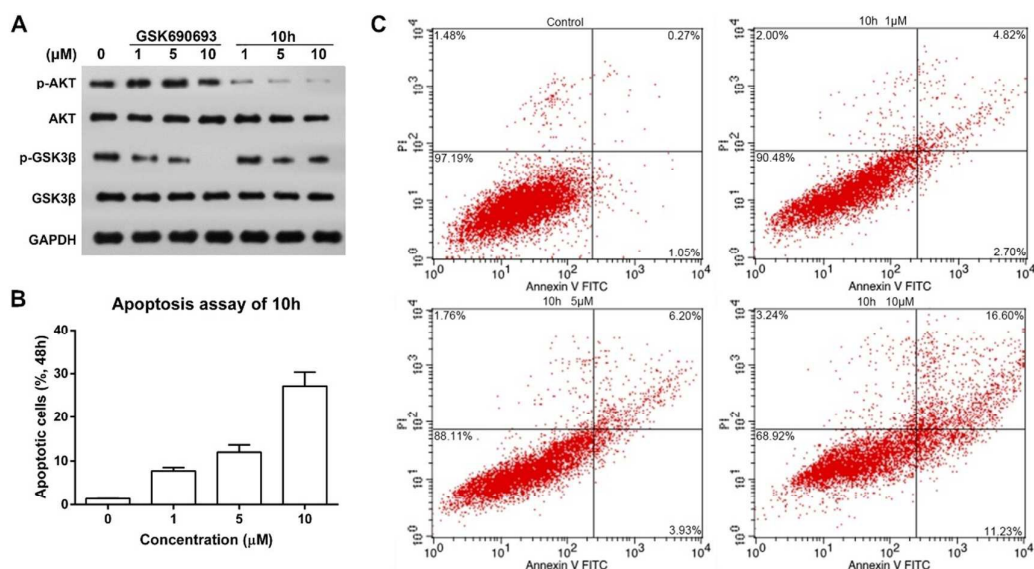


Figure 4. (A) Effects of **10h** on AKT signaling within PC-3 cells; (B-C) Apoptosis induction by **10h** in PC-3 cells.

2.5. Apoptotic induction of 10h in PC-3 cells

Compound **10h** was further evaluated for its apoptosis inductive effect in PC-3 cells *via* an annexin V-FITC/propidium iodide (PI)-binding assay (Figure 4B-C). After 48 hours of the treatment, a mild degree of apoptosis was observed in a dose-dependent manner. The percentage of apoptotic cells increased by 1.32%-27.83% when compared to the DMSO control.

2.6. Stability in human liver microsomes

Liver microsomes are subcellular fractions derived from the endoplasmic reticulum of liver, they contain a variety of metabolic enzymes (cytochrome P450) and are used as an *in vitro* model for the prediction of *in vivo* metabolic stability in liver. Compound **10h** showed high metabolic stability with a more than 80% total remaining after an one-hour treatment in human liver microsomes. The calculated half-life ($T_{1/2}$) and clearance rate ($CL_{int(mic)}$) were more than 145 min and less than 9.6 $\mu\text{L}/\text{min}/\text{mg}$, respectively (Table 2).

Table 2. Metabolic stability of **10h** in human liver microsomes.

Code	$T_{1/2}$ (min)	$CL_{int(mic)}$ ($\mu\text{L}/\text{min}/\text{mg}$)	$CL_{int(liver)}$ ($\text{mL}/\text{min}/\text{kg}$)	Remaining (T = 60min)

10h	> 145	< 9.6	< 8.6	81.8%
Testosterone	16.9	82.2	74.0	8.1%
Diclofenac	10.2	136.2	122.6	1.5%
Propafenone	7.7	180.9	162.8	0.5%

3. Conclusion

In this work, the discovery of a potent AKT targeted inhibitor **10h** showing efficient anti-prostate cancer potency in PC-3 cells was described. This compound belonged to a series of *N*-heterocyclic based AKT1 inhibitors with the structural feature of a piperidin-4-yl side chain. Compounds based on a 3-halogenic pyrazolopyrimidine ring in this series showed high AKT1 inhibition and potent anti-proliferative effect in PC-3 cells, of which **10h** showed the highest potency on both AKT1 inhibition ($IC_{50} = 24.3$ nM) and PC-3 cell proliferation ($IC_{50} = 3.7$ μ M). In a further characterization of kinase selectivity profile, compound **10h** showed potent pan-AKT inhibitory activity, as well as inhibitory activity against kinases of AGC family. **10h** could moderately inhibit cellular AKT phosphorylation and induce apoptosis of PC-3 cells. It also showed high metabolic stability in human liver microsomes. Therefore, further evaluation of **10h** was warranted for its potential application as an anti-prostate cancer therapeutic.

4. Materials and methods

4.1. Chemistry

All reagents and solvents were purchased from commercial suppliers and used without further purification. All reactions were monitored by thin layer chromatography (TLC), silica gel GF254 plates were used and visualized with UV light. Column chromatography was performed with silica gel using the solvent systems as indicated in the synthetic procedures. NMR spectra were recorded on a Bruker AVANCE DRX400 or DRX600 spectrometer using tetramethylsilane (TMS) as an internal standard in DMSO- d_6 . Chemical shifts are reported in parts per million (ppm). Coupling constants (*J*) are given in Hz. The mass spectra (MS) were measured with an API 4000. All of the melting points were determined using a Büchi capillary

melting point apparatus and were uncorrected.

4.1.1. General procedure for the synthesis of intermediate 2

To a solution of 4-chloro-1*H*-pyrazolo[3,4-*d*]pyrimidine (**1**, 3.1 g, 20.0 mmol) in *N,N*-dimethylformamide (DMF, 15 ml), *N*-chlorosuccinimide (NCS, 2.8 g, 21.0 mmol) or *N*-bromosuccinimide (NBS, 3.7 g, 21.0 mmol) was added. This mixture was stirred at room temperature for 12-18 hours. Icy water (150 ml) was poured into the reaction mixture, and the precipitate was filtered, washed with water (2 × 20 ml), and dried to give intermediate **2**.

3,4-Dichloro-1*H*-pyrazolo[3,4-*d*]pyrimidine (**2a**)

Light yellow solid, yield 74%. ¹H NMR (400 MHz, DMSO-*d*₆) δ 14.77 (s, 1H), 8.88 (s, 1H).

3-Bromo-4-chloro-1*H*-pyrazolo[3,4-*d*]pyrimidine (**2b**)

Off-white solid, yield 94%. ¹H NMR (400 MHz, DMSO-*d*₆) δ 14.13 (s, 1H), 8.06 (s, 1H).

4.1.2. General procedure for the synthesis of intermediates 3, 12 and 16

A solution of intermediate **2** (15.2 mmol), *N,N*-diisopropylethylamine (DIPEA, 4.0 g, 30.4 mmol) and *tert*-butyl piperazine-1-carboxylate (3.1 g, 16.7 mmol) in DMF (15 ml) was heated at 150 °C under microwave irradiation for 20 min. This reaction mixture was cooled down and poured into ice-cold water (150 ml), followed by extraction of ethyl acetate (EA, 3 × 30 ml). The organic extracts were combined, washed by saturated aqueous NH₄Cl (2 × 30 ml) and brine (2 × 30 ml), dried over anhydrous Na₂SO₄, filtered, condensed under reduced pressure, and purified by column chromatography (petroleum ether (PE)/EA = 9/1) to get intermediate **3**.

Intermediates **12** and **16** were prepared in a similar procedure as described above using the commercially available 6-chloro-9*H*-purine (**11**) and 4-chloroquinazoline (**15**) as starting materials, respectively.

Tert-butyl 4-(9*H*-purin-6-yl)piperazine-1-carboxylate (**12**)

Off-white solid, yield 91%. ¹H NMR (400 MHz, DMSO-*d*₆) δ 13.09 (s, 1H), 8.23 (s, 1H), 8.15 (s, 1H), 4.21 (br s, 4H), 3.44 (br s, 4H), 1.43 (s, 9H).

Tert-butyl 4-(quinazolin-4-yl)piperazine-1-carboxylate (**16**)

Off-white solid, yield 88%. ^1H NMR (400 MHz, $\text{DMSO-}d_6$) δ 8.88 (s, 1H), 8.24 (d, $J = 8.4$ Hz, 1H), 8.09–7.93 (m, 2H), 7.72 (t, $J = 7.7$ Hz, 1H), 7.49–7.15 (m, 1H), 4.26–4.14 (m, 4H), 3.62 (br s, 4H), 1.44 (s, 9H).

4.1.3. General procedure for the synthesis of intermediates 4, 13 and 17

To a solution of intermediate **3** (1.0 mmol) in dichloromethane (DCM, 6 ml), trifluoroacetic acid (TFA, 2 ml) was added. This mixture was stirred at room temperature for 4 hours, and the precipitate formed was collected by filtration and dried to give intermediate **4**. Intermediates **13** and **17** were prepared in a similar procedure as described above.

3-Chloro-4-(piperazin-1-yl)-1*H*-pyrazolo[3,4-*d*]pyrimidine (**4a**)

Off-white solid, yield 68%. ^1H NMR (400 MHz, $\text{DMSO-}d_6$) δ 8.36 (d, $J = 5.7$ Hz, 1H), 3.93–3.79 (m, 4H), 3.12–3.00 (m, 4H).

3-Bromo-4-(piperazin-1-yl)-1*H*-pyrazolo[3,4-*d*]pyrimidine (**4b**)

Off-white solid, yield 88%. ^1H NMR (400 MHz, $\text{DMSO-}d_6$) δ 8.38 (s, 1H), 3.96–3.74 (m, 4H), 3.20–3.07 (m, 4H).

4-(Piperazin-1-yl)-1*H*-pyrazolo[3,4-*d*]pyrimidine (**4c**)

Off-white solid, yield 84%. ^1H NMR (400 MHz, $\text{DMSO-}d_6$) δ 9.99 (s, 2H), 8.97 (s, 1H), 8.63 (s, 1H), 4.32 (s, 4H), 3.35 (s, 4H).

6-(Piperazin-1-yl)-9*H*-purine dihydrochloride (**13**)

Off-white solid, yield 88%. ^1H NMR (400 MHz, $\text{DMSO-}d_6$) δ 9.71 (br s, 2H), 8.45 (s, 1H), 8.39 (s, 1H), 4.52 (s, 4H), 3.28 (s, 4H).

4-(Piperazin-1-yl)quinazoline dihydrochloride (**17**)

Off-white solid, yield 84%. ^1H NMR (400 MHz, $\text{DMSO-}d_6$) δ 10.02 (s, 2H), 8.95 (s, 1H), 8.25 (d, $J = 8.4$ Hz, 1H), 8.10–8.02 (m, 2H), 7.74 (ddd, $J = 8.4, 5.6, 2.7$ Hz, 1H), 4.37 (s, 4H), 3.34 (s, 4H).

4.1.4. General procedure for the synthesis of intermediate 8

To a solution of bis(2-chloroethyl)amine hydrochloride (**7**, 8.0 g, 44.8 mmol) in DCM (20 ml) at room temperature, aqueous NaOH (6 M, 20 ml) was added, followed by addition of Boc_2O (9.8 g, 44.8 mmol). After addition, the reaction mixture was stirred for 12 hours, and extracted with DCM (2×30 ml). The organic extracts were

combined, washed by brine (30 ml), dried over Na₂SO₄, filtered and concentrated under reduced pressure to give a colorless oil as intermediate **8** which was used directly for next step without further purification.

4.1.5. General procedure for the synthesis of intermediate **9**

To a solution of substituted phenylacetonitrile **6** (14.8 mmol) and intermediate **8** (16.3 mmol) in DMF (25 mL) on an ice bath, sodium hydride (1.1 g, 44.4 mmol) was added in portion. After addition, the reaction mixture was heated at 80 °C for 12-18 hours. This mixture was then cooled down and quenched by dropwise addition of H₂O (20 ml). After extraction with EA (3 × 30 ml), the organic extracts were combined, washed with brine (2 × 30 ml), dried over Na₂SO₄, filtered, concentrated under reduced pressure, and purified using column chromatography (PE/EA = 20/1) to afford intermediate **9**.

***Tert*-butyl 4-cyano-4-(4-fluorophenyl)piperidine-1-carboxylate (9a)**

White solid, yield 43%. ¹H NMR (400 MHz, DMSO-*d*₆) δ 7.43 (s, 4H), 3.76 (d, *J* = 13.6 Hz, 2H), 2.98 (br s, 2H), 2.33 (d, *J* = 13.6 Hz, 2H), 1.76–1.68 (m, 2H), 1.39 (s, 9H).

***Tert*-butyl 4-(4-chlorophenyl)-4-cyanopiperidine-1-carboxylate (9b)**

White solid, yield 52%. ¹H NMR (600 MHz, DMSO-*d*₆) δ 7.57 (d, *J* = 8.4 Hz, 2H), 7.52 (d, *J* = 8.4 Hz, 2H), 4.13 (br s, 2H), 3.01 (br s, 2H), 2.11 (d, *J* = 13.2 Hz, 2H), 1.90 (td, *J* = 12.9, 4.2 Hz, 2H), 1.41 (s, 9H).

***Tert*-butyl 4-(4-bromophenyl)-4-cyanopiperidine-1-carboxylate (9c)**

White solid, yield 40%. ¹H NMR (400 MHz, DMSO-*d*₆) δ 7.64 (d, *J* = 8.6 Hz, 2H), 7.53 (d, *J* = 8.6 Hz, 2H), 4.12 (d, *J* = 12.8 Hz, 2H), 3.01 (br s, 2H), 2.12 (d, *J* = 12.8 Hz, 2H), 1.90 (td, *J* = 13.1, 4.2 Hz, 2H), 1.41 (s, 9H).

4.1.6. General procedure for the synthesis of intermediate **5**

To a solution of intermediate **9** (6.6 mmol) in ethanol (10 ml), aqueous NaOH (10 M, 10 ml) was added. The reaction mixture was stirred at 60 °C for 48 hours, cooled down and concentrated under reduced pressure. The residue was adjusted by aqueous HCl (1 M) to pH 5-6, and white solid precipitate was collected by filtration, washed with H₂O (2 × 30 ml), and dried to afford the intermediate **5**.

1-(*Tert*-butoxycarbonyl)-4-(4-fluorophenyl)piperidine-4-carboxylic acid (5a)

White solid, yield 86%. ¹H NMR (400 MHz, DMSO-*d*₆) δ 12.82 (s, 1H), 7.43 (s, 4H), 3.77 (d, *J* = 13.6 Hz, 2H), 2.97 (br s, 2H), 2.34 (d, *J* = 13.6 Hz, 2H), 1.77–1.69 (m, 2H), 1.39 (s, 9H).

1-(*Tert*-butoxycarbonyl)-4-(4-chlorophenyl)piperidine-4-carboxylic acid (5b)

White solid, yield 75%. ¹H NMR (400 MHz, DMSO-*d*₆) δ 12.81 (s, 1H), 7.42 (s, 4H), 3.76 (d, *J* = 13.6 Hz, 2H), 2.98 (br s, 2H), 2.33 (d, *J* = 13.6 Hz, 2H), 1.74–1.68 (m, 2H), 1.40 (s, 9H).

4-(4-Bromophenyl)-1-(*tert*-butoxycarbonyl)piperidine-4-carboxylic acid (5c)

White solid, yield 87%. ¹H NMR (600 MHz, DMSO-*d*₆) δ 12.80 (s, 1H), 7.54 (d, *J* = 8.4 Hz, 2H), 7.36 (d, *J* = 8.4 Hz, 2H), 3.76 (d, *J* = 13.8 Hz, 2H), 2.97 (br s, 2H), 2.34 (d, *J* = 13.8 Hz, 2H), 1.72–1.66 (m, 2H), 1.41 (s, 9H).

4.1.7. General procedure for the synthesis of compounds 10, 14 and 18

To a solution of intermediate **5** (1.0 mmol) in DCM (6 ml), HBTU (417 mg, 1.1 mmol) and DIPEA (388 mg, 3.0 mmol) were added. After stirring at room temperature for 15 min, intermediate **4** (1.0 mmol) was added. This reaction mixture was stirred for 6 hours and washed with saturated NH₄Cl (3 × 20 ml) and brine (30 ml). The organic layer was concentrated under reduced pressure to give an oily residue. This residue was dissolved in DCM (4 ml), and TFA (2 ml) was added. After stirring for 4 hours at room temperature, the mixture was concentrated under reduced pressure, adjusted with saturated Na₂CO₃ to pH = 9, and extracted with DCM (3 × 20 ml). The organic extracts were combined, washed with brine (2 × 20 ml), and concentrated under reduced pressure to give a solid residue which was purified by column chromatography (DCM/MeOH = 50/1 ramping to 20/1) to give compounds **10a-10l**. Compounds **14a-14d** and **18a-18d** were prepared in a similar procedure as mentioned above.

(4-(1*H*-pyrazolo[3,4-*d*]pyrimidin-4-yl)piperazin-1-yl)(4-(4-fluorophenyl)piperidin-4-yl)methanone (10a)

White solid, yield 64%. Mp: 112–115 °C. ¹H NMR (400 MHz, CD₃OD) δ 8.20 (s, 1H), 8.11 (s, 1H), 7.36 (dd, *J* = 8.5, 5.2 Hz, 2H), 7.14 (t, *J* = 8.6 Hz, 2H), 3.69 (br s, 8H),

2.38 (d, $J = 13.3$ Hz, 2H), 2.05–1.84 (m, 2H). ^{13}C NMR (100 MHz, CD_3OD) δ 173.46, 157.08, 155.04, 154.69, 140.40, 133.41, 126.93, 115.80, 115.58, 99.78, 49.11, 43.92, 42.77, 35.57. HRMS (ESI) m/z calculated for $\text{C}_{21}\text{H}_{25}\text{FN}_7\text{O}$ $[\text{M}+\text{H}]^+$: 410.2099, found 410.2098.

(4-(1*H*-pyrazolo[3,4-*d*]pyrimidin-4-yl)piperazin-1-yl)(4-(4-chlorophenyl)piperidin-4-yl)methanone (10b)

White solid, yield 67%. Mp: 120–123 °C. ^1H NMR (400 MHz, CD_3OD) δ 8.21 (s, 1H), 8.12 (s, 1H), 7.42 (d, $J = 8.3$ Hz, 2H), 7.34 (d, $J = 8.3$ Hz, 2H), 4.05–3.45 (m, 8H), 3.20–3.04 (m, 4H), 2.42 (d, $J = 13.5$ Hz, 2H), 2.01 (br s, 2H). ^{13}C NMR (100 MHz, MeOD) δ 172.82, 157.09, 155.04, 154.70, 142.69, 133.40, 132.97, 129.19, 126.69, 99.79, 48.88, 43.84, 42.43, 34.52. HRMS (ESI) m/z calculated for $\text{C}_{21}\text{H}_{25}\text{ClN}_7\text{O}$ $[\text{M}+\text{H}]^+$: 426.1804, found 426.1799.

(4-(1*H*-pyrazolo[3,4-*d*]pyrimidin-4-yl)piperazin-1-yl)(4-(4-bromophenyl)piperidin-4-yl)methanone (10c)

White solid, yield 62%. Mp: 149–152 °C. ^1H NMR (400 MHz, CD_3OD) δ 8.21 (s, 1H), 8.12 (s, 1H), 7.55 (d, $J = 8.6$ Hz, 2H), 7.27 (d, $J = 8.6$ Hz, 2H), 3.67 (br s, 8H), 3.04 (br s, 4H), 2.37 (d, $J = 12.9$ Hz, 2H), 1.95 (t, $J = 14.7$ Hz, 2H). ^{13}C NMR (100 MHz, MeOD) δ 173.17, 157.09, 155.04, 154.69, 143.66, 133.42, 132.12, 127.06, 120.63, 99.79, 49.31, 43.33, 41.81, 35.35. HRMS (ESI) m/z calculated for $\text{C}_{21}\text{H}_{25}\text{BrN}_7\text{O}$ $[\text{M}+\text{H}]^+$: 472.1278, found 472.1282.

(4-(1*H*-pyrazolo[3,4-*d*]pyrimidin-4-yl)piperazin-1-yl)(4-(3,4-dichlorophenyl)piperidin-4-yl)methanone (10d)

White solid, yield 52%. Mp: 174–177 °C. ^1H NMR (400 MHz, CD_3OD) δ 8.20 (d, $J = 10.6$ Hz, 1H), 8.13 (s, 1H), 7.55 (d, $J = 8.5$ Hz, 1H), 7.51 (d, $J = 1.9$ Hz, 1H), 7.26 (dd, $J = 8.4, 1.9$ Hz, 1H), 3.80 (br s, 4H), 3.55 (br s, 4H), 3.14–3.01 (m, 4H), 2.39 (d, $J = 13.3$ Hz, 2H), 2.02–1.92 (m, 2H). ^{13}C NMR (100 MHz, MeOD) δ 172.43, 157.08, 155.04, 154.70, 144.94, 133.47, 132.98, 131.14, 130.92, 127.07, 125.18, 99.80, 49.12, 45.46, 42.53, 34.91. HRMS (ESI) m/z calculated for $\text{C}_{21}\text{H}_{24}\text{Cl}_2\text{N}_7\text{O}$ $[\text{M}+\text{H}]^+$: 460.1414, found 460.1409.

(4-(3-Chloro-1*H*-pyrazolo[3,4-*d*]pyrimidin-4-yl)piperazin-1-yl)(4-(4-fluorophenyl

)piperidin-4-yl)methanone (10e)

Off-white solid, yield 53%. Mp: 135–138 °C. ¹H NMR (400 MHz, DMSO-*d*₆) δ 8.21 (s, 1H), 7.35–7.27 (m, 2H), 7.21 (t, *J* = 8.7 Hz, 2H), 3.42 (br s, 8H), 2.82 (d, *J* = 13.2 Hz, 4H), 2.18 (d, *J* = 12.8 Hz, 2H), 1.84–1.67 (m, 2H). ¹³C NMR (100 MHz, DMSO-*d*₆) δ 172.62, 162.37, 159.95, 158.41, 154.14, 141.96, 129.69, 127.67, 116.29, 116.08, 98.88, 49.51, 48.06, 43.76, 41.09, 37.08. HRMS (ESI) *m/z* calculated for C₂₁H₂₄ClFN₇O [M+H]⁺: 444.1709, found 444.1710.

(4-(3-Chloro-1*H*-pyrazolo[3,4-*d*]pyrimidin-4-yl)piperazin-1-yl)(4-(4-chlorophenyl)piperidin-4-yl)methanone (10f)

White solid, yield 51%. Mp: 184–188 °C. ¹H NMR (400 MHz, DMSO-*d*₆) δ 8.23 (s, 1H), 7.44 (d, *J* = 8.5 Hz, 2H), 7.30 (d, *J* = 8.5 Hz, 2H), 3.44 (br s, 8H), 2.82 (d, *J* = 15.6 Hz, 4H), 2.17 (d, *J* = 12.9 Hz, 2H), 1.76 (d, *J* = 7.5 Hz, 2H). ¹³C NMR (100 MHz, DMSO-*d*₆) δ 172.52, 158.34, 158.10, 154.50, 144.71, 131.60, 130.10, 129.43, 127.68, 98.94, 49.65, 47.96, 43.70, 41.08, 36.84. HRMS (ESI) *m/z* calculated for C₂₁H₂₄Cl₂N₇O [M+H]⁺: 460.1414, found 460.1416.

(4-(4-Bromophenyl)piperidin-4-yl)(4-(3-chloro-1*H*-pyrazolo[3,4-*d*]pyrimidin-4-yl)piperazin-1-yl)methanone (10g)

White solid, yield 56%. Mp: 181–185 °C. ¹H NMR (400 MHz, DMSO-*d*₆) δ 8.10 (s, 1H), 7.57 (d, *J* = 8.1 Hz, 2H), 7.24 (d, *J* = 8.2 Hz, 2H), 3.41 (br s, 8H), 2.82 (br s, 4H), 2.15 (d, *J* = 12.7 Hz, 2H), 1.73 (d, *J* = 9.7 Hz, 2H). ¹³C NMR (100 MHz, DMSO-*d*₆) δ 172.45, 160.45, 158.41, 152.79, 144.79, 135.71, 132.41, 128.05, 127.84, 98.77, 49.70, 48.26, 43.84, 40.83, 36.99. HRMS (ESI) *m/z* calculated for C₂₁H₂₄ClBrN₇O [M+H]⁺: 504.0909, found 504.0904.

(4-(3-Chloro-1*H*-pyrazolo[3,4-*d*]pyrimidin-4-yl)piperazin-1-yl)(4-(3,4-dichlorophenyl)piperidin-4-yl)methanone (10h)

Off-white solid, yield 49%. Mp: 195–199 °C. ¹H NMR (400 MHz, CD₃OD) δ 8.22 (d, *J* = 15.1 Hz, 1H), 7.56 (d, *J* = 8.4 Hz, 1H), 7.51 (s, 1H), 7.27 (d, *J* = 6.8 Hz, 1H), 3.61 (br s, 8H), 3.08 (br s, 4H), 2.39 (d, *J* = 13.4 Hz, 2H), 1.96 (br s, 2H). ¹³C NMR (100 MHz, MeOD) δ 172.31, 158.46, 154.59, 144.99, 132.97, 131.17, 131.14, 130.94, 127.14, 125.19, 122.38, 98.78, 49.19, 49.05, 42.55, 42.47, 34.84. HRMS (ESI) *m/z*

calculated for C₂₁H₂₃Cl₃N₇O [M+H]⁺: 494.1024, found 494.1024.

(4-(3-Bromo-1*H*-pyrazolo[3,4-*d*]pyrimidin-4-yl)piperazin-1-yl)(4-(4-fluorophenyl)piperidin-4-yl)methanone (10i)

Off-white solid, yield 32%. Mp: 194–196 °C. ¹H NMR (400 MHz, DMSO-*d*₆) δ 8.27 (s, 1H), 7.31–7.21 (m, 4H), 3.42 (br s, 8H), 2.87 (br s, 4H), 2.17 (s, 2H), 1.78 (s, 2H). ¹³C NMR (100 MHz, DMSO-*d*₆) δ 172.63, 158.88, 157.61, 154.74, 141.82, 127.65, 118.64, 117.03, 116.23, 101.59, 49.40, 48.75, 43.63, 36.77. HRMS (ESI) *m/z* calculated for C₂₁H₂₄BrFN₇O [M+H]⁺: 490.1184, found 490.1186.

(4-(3-Bromo-1*H*-pyrazolo[3,4-*d*]pyrimidin-4-yl)piperazin-1-yl)(4-(4-chlorophenyl)piperidin-4-yl)methanone (10j)

Off-white solid, yield 43%. Mp: 180–184 °C. ¹H NMR (400 MHz, CD₃OD) δ 8.27 (s, 1H), 7.48 (d, *J* = 8.4 Hz, 2H), 7.37 (d, *J* = 8.5 Hz, 2H), 3.96–3.59 (m, 4H), 3.43 (d, *J* = 12.9 Hz, 2H), 3.36 (d, *J* = 12.0 Hz, 2H), 3.21 (q, *J* = 7.3 Hz, 4H), 2.57 (d, *J* = 13.9 Hz, 2H), 2.17 (t, *J* = 11.6 Hz, 2H). ¹³C NMR (100 MHz, DMSO-*d*₆) δ 171.16, 158.80, 157.01, 155.13, 142.52, 132.36, 129.77, 127.52, 119.08, 101.59, 48.02, 45.91, 41.54, 32.21. HRMS (ESI) *m/z* calculated for C₂₁H₂₄BrClN₇O [M+H]⁺: 506.0888, found 506.0898.

(4-(3-Bromo-1*H*-pyrazolo[3,4-*d*]pyrimidin-4-yl)piperazin-1-yl)(4-(4-bromophenyl)piperidin-4-yl)methanone (10k)

White solid, yield 52%. Mp: 175–178 °C. ¹H NMR (400 MHz, CD₃OD) δ 8.26 (s, 1H), 7.62 (d, *J* = 8.5 Hz, 2H), 7.32 (d, *J* = 8.5 Hz, 2H), 3.96 – 3.59 (m, 4H), 3.46 – 3.35 (m, 4H), 3.21 (q, *J* = 7.3 Hz, 4H), 2.56 (d, *J* = 13.8 Hz, 2H), 2.19 (t, *J* = 11.5 Hz, 2H). ¹³C NMR (100 MHz, MeOD) δ 171.48, 158.91, 156.41, 154.62, 141.99, 132.44, 126.96, 121.34, 119.03, 101.53, 47.93, 46.51, 41.70, 38.90, 32.07. HRMS (ESI) *m/z* calculated for C₂₁H₂₄Br₂N₇O [M+H]⁺: 550.0383, found 550.0393.

(4-(3-Bromo-1*H*-pyrazolo[3,4-*d*]pyrimidin-4-yl)piperazin-1-yl)(4-(3,4-dichlorophenyl)piperidin-4-yl)methanone (10l)

Hoary solid, yield 34%. Mp: 195–198 °C. ¹H NMR (400 MHz, CD₃OD) δ 8.27 (s, 1H), 7.60 (d, *J* = 8.5 Hz, 1H), 7.53 (d, *J* = 2.2 Hz, 1H), 7.29 (dd, *J* = 8.5, 2.2 Hz, 1H), 3.66 (br s, 8H), 3.28 (br s, 2H), 3.21 (t, *J* = 11.8 Hz, 2H), 2.49 (d, *J* = 13.4 Hz, 2H),

2.08 (t, $J = 15.2$ Hz, 2H). ^{13}C NMR (100 MHz, MeOD) δ 171.49, 158.97, 156.50, 154.56, 144.10, 133.13, 131.31, 127.08, 125.16, 118.95, 101.57, 48.36, 47.05, 45.26, 41.94, 33.24. HRMS (ESI) m/z calculated for $\text{C}_{21}\text{H}_{23}\text{BrCl}_2\text{N}_7\text{O}$ $[\text{M}+\text{H}]^+$: 540.0499, found 540.0510.

(4-(9H-purin-6-yl)piperazin-1-yl)(4-(4-fluorophenyl)piperidin-4-yl)methanone

(14a)

White solid, yield 59%. Mp: 173–175 °C. ^1H NMR (400 MHz, DMSO- d_6) δ 8.19 (s, 1H), 8.11 (s, 1H), 7.61 (d, $J = 8.4$ Hz, 2H), 7.25 (d, $J = 8.4$ Hz, 2H), 3.90 (br s, 4H), 3.39 (br s, 4H), 3.10 (d, $J = 12.5$ Hz, 2H), 2.96 (t, $J = 11.7$ Hz, 2H), 2.29 (d, $J = 13.3$ Hz, 2H), 1.99 (t, $J = 11.0$ Hz, 2H). ^{13}C NMR (100 MHz, DMSO- d_6) δ 171.63, 153.55, 152.07, 143.98, 138.97, 132.51, 127.97, 120.46, 119.26, 48.77, 44.51, 44.42, 44.18, 42.47, 34.17. HRMS (ESI) m/z calculated for $\text{C}_{21}\text{H}_{25}\text{FN}_7\text{O}$ $[\text{M}+\text{H}]^+$: 410.2099, found 410.2097.

(4-(9H-purin-6-yl)piperazin-1-yl)(4-(4-chlorophenyl)piperidin-4-yl)methanone

(14b)

White solid, yield 63%. Mp: 186–188 °C. ^1H NMR (400 MHz, DMSO- d_6) δ 8.18 (s, 1H), 8.10 (s, 1H), 7.34 (dd, $J = 8.8, 5.3$ Hz, 2H), 7.26 (t, $J = 8.8$ Hz, 2H), 4.28–3.69 (m, 6H), 3.58–3.41 (m, 2H), 3.21 (d, $J = 12.8$ Hz, 2H), 3.03 (t, $J = 11.7$ Hz, 2H), 2.36 (d, $J = 13.7$ Hz, 2H), 2.09 (t, $J = 12.3$ Hz, 2H). ^{13}C NMR (100 MHz, DMSO) δ 171.52, 162.65, 160.22, 153.48, 152.14, 140.24, 138.96, 127.66, 119.26, 116.59, 116.38, 48.15, 46.08, 44.59, 44.40, 43.12, 41.96, 33.25. HRMS (ESI) m/z calculated for $\text{C}_{21}\text{H}_{25}\text{ClN}_7\text{O}$ $[\text{M}+\text{H}]^+$: 426.1804, found 426.1806.

(4-(9H-purin-6-yl)piperazin-1-yl)(4-(4-bromophenyl)piperidin-4-yl)methanone

(14c)

White solid, yield 67%. Mp: 234–236 °C. ^1H NMR (400 MHz, DMSO- d_6) δ 8.18 (s, 1H), 8.10 (s, 1H), 7.46 (d, $J = 8.4$ Hz, 2H), 7.31 (d, $J = 8.4$ Hz, 2H), 3.88 (br s, 4H), 3.39 (br s, 4H), 3.01–2.83 (m, 4H), 2.23 (d, $J = 13.1$ Hz, 2H), 1.86 (t, $J = 10.0$ Hz, 2H). ^{13}C NMR (100 MHz, DMSO- d_6) δ 172.08, 153.48, 152.07, 144.18, 138.97, 131.75, 129.50, 127.67, 119.25, 49.18, 44.82, 44.49, 44.28, 43.12, 35.66. HRMS (ESI) m/z calculated for $\text{C}_{21}\text{H}_{25}\text{BrN}_7\text{O}$ $[\text{M}+\text{H}]^+$: 472.1278, found 472.1279.

(4-(9H-purin-6-yl)piperazin-1-yl)(4-(3,4-dichlorophenyl)piperidin-4-yl)methanone (14d)

White solid, yield 69%. Mp: 203–205 °C. ¹H NMR (400 MHz, DMSO-*d*₆) δ 8.19 (s, 1H), 8.11 (s, 1H), 7.64 (d, *J* = 8.4 Hz, 1H), 7.50 (s, 1H), 7.24 (d, *J* = 9.9 Hz, 1H), 3.93 (br s, 8H), 2.95–2.78 (m, 4H), 2.20 (d, *J* = 13.0 Hz, 2H), 1.79 (d, *J* = 13.4 Hz, 2H). ¹³C NMR (100 MHz, DMSO-*d*₆) δ 171.84, 153.46, 152.08, 146.64, 139.03, 132.14, 131.63, 129.72, 127.66, 126.52, 119.27, 49.58, 46.15, 44.61, 43.44, 36.39. HRMS (ESI) *m/z* calculated for C₂₁H₂₄Cl₂N₇O [M+H]⁺: 460.1414, found 460.1411.

(4-(4-Fluorophenyl)piperidin-4-yl)(4-(quinazolin-4-yl)piperazin-1-yl)methanone (18a)

White solid, yield 67%. Mp: 145–147 °C. ¹H NMR (400 MHz, DMSO-*d*₆) δ 8.61 (s, 1H), 7.94 (d, *J* = 8.3 Hz, 1H), 7.81 (s, 2H), 7.63 (d, *J* = 8.4 Hz, 2H), 7.53 (s, 1H), 7.24 (d, *J* = 8.4 Hz, 2H), 3.91–3.45 (m, 6H), 3.41–3.35 (m, 2H), 3.25 (d, *J* = 12.6 Hz, 2H), 3.05 (t, *J* = 12.1 Hz, 2H), 2.34 (d, *J* = 13.6 Hz, 2H), 2.14 (t, *J* = 11.7 Hz, 2H). ¹³C NMR (100 MHz, DMSO-*d*₆) δ 171.08, 164.10, 153.95, 151.69, 143.15, 133.31, 132.74, 128.50, 127.71, 126.28, 125.54, 120.72, 116.06, 49.09, 48.06, 41.66, 32.56. HRMS (ESI) *m/z* calculated for C₂₄H₂₇FN₅O [M+H]⁺: 420.2194, found 420.2189.

(4-(4-Chlorophenyl)piperidin-4-yl)(4-(quinazolin-4-yl)piperazin-1-yl)methanone (18b)

Off-white solid, yield 64%. Mp: 106–108 °C. ¹H NMR (400 MHz, DMSO-*d*₆) δ 8.60 (s, 1H), 7.93 (d, *J* = 8.2 Hz, 1H), 7.80 (s, 2H), 7.52 (s, 1H), 7.38–7.16 (m, 4H), 3.80–3.41 (m, 6H), 3.26–3.17 (m, 4H), 3.03 (t, *J* = 11.9 Hz, 2H), 2.34 (d, *J* = 13.3 Hz, 2H), 2.08 (t, *J* = 11.8 Hz, 2H). ¹³C NMR (100 MHz, DMSO-*d*₆) δ 171.53, 164.11, 153.95, 151.65, 140.21, 133.30, 128.50, 127.54, 126.27, 125.69, 116.65, 116.44, 116.29, 48.99, 48.83, 48.20, 41.97, 33.27. HRMS (ESI) *m/z* calculated for C₂₄H₂₇ClN₅O [M+H]⁺: 436.1899, found 436.1902.

(4-(4-Bromophenyl)piperidin-4-yl)(4-(quinazolin-4-yl)piperazin-1-yl)methanone (18c)

White solid, yield 72%. Mp: 189–191 °C. ¹H NMR (400 MHz, DMSO-*d*₆) δ 8.61 (s, 1H), 7.94 (d, *J* = 8.3 Hz, 1H), 7.84–7.78 (m, 2H), 7.57–7.45 (m, 3H), 7.31 (d, *J* = 8.6

Hz, 2H), 3.92–3.38 (m, 6H), 3.26 (br s, 4H), 3.07 (t, $J = 12.0$ Hz, 2H), 2.36 (d, $J = 13.8$ Hz, 2H), 2.17 (t, $J = 11.8$ Hz, 2H). ^{13}C NMR (100 MHz, DMSO) δ 171.15, 164.09, 153.94, 151.66, 142.67, 133.29, 132.29, 129.77, 128.50, 127.44, 126.27, 125.69, 116.29, 48.92, 48.11, 41.58, 32.38. HRMS (ESI) m/z calculated for $\text{C}_{24}\text{H}_{27}\text{BrN}_5\text{O}$ $[\text{M}+\text{H}]^+$: 482.1373, found 482.1374.

(4-(3,4-Dichlorophenyl)piperidin-4-yl)(4-(quinazolin-4-yl)piperazin-1-yl)methanone (18d)

White solid, yield 76%. Mp: 254–256 °C. ^1H NMR (400 MHz, DMSO- d_6) δ 8.61 (s, 1H), 7.95 (d, $J = 8.3$ Hz, 1H), 7.83–7.79 (m, 2H), 7.69 (d, $J = 8.5$ Hz, 1H), 7.56–7.48 (m, 2H), 7.25 (dd, $J = 8.5, 2.2$ Hz, 1H), 3.94–3.31 (m, 7H), 3.27 (br s, 3H), 3.06 (t, $J = 12.0$ Hz, 2H), 2.37 (d, $J = 13.8$ Hz, 2H), 2.18 (t, $J = 11.6$ Hz, 2H). ^{13}C NMR (100 MHz, DMSO) δ 170.67, 164.09, 153.94, 151.68, 144.67, 133.29, 132.44, 131.96, 130.47, 128.51, 127.43, 126.32, 126.29, 125.69, 116.31, 49.00, 48.98, 48.17, 41.56, 32.31. HRMS (ESI) m/z calculated for $\text{C}_{24}\text{H}_{26}\text{Cl}_2\text{N}_5\text{O}$ $[\text{M}+\text{H}]^+$: 470.1509, found 470.1506.

4.2. *In vitro* kinase assay

In vitro AKT1 kinase inhibitory activity was evaluated *via* a Homogeneous Time-Resolved Fluorescence (HTRF) assay (LANCER) using an AKT kinase kit (Cisbio) in a 384-well plate. Each well was added subsequently with AKT1, STK substrate-biotin, tested compounds and ATP in kinase buffer (50 mM HEPES, 5 mM MgCl_2 , 1 mM DTT, 0.02% NaN_3 and 0.01% BSA, pH 7.0), and incubated for 45 minutes at 25 °C. Finally, Sa-XL665 and STK Ab-Cryptate were added to stop the enzymatic step and further incubated for 2 hours to finish the detection process. The ratio (665 nm/620 nm) was obtained using a microplate reader (Perkin Elmer, USA).

4.3. Cell proliferation assays (MTT)

Human prostate cancer cell line PC-3 was purchased from the American type culture collection (ATCC), and cultured in RPMI 1640 medium containing 10% fetal bovine serum (Gibco, USA) and 100 IU/mL penicillin and 100 $\mu\text{g}/\text{mL}$ streptomycin in a humidified atmosphere with 5% CO_2 at 37°C. All the compounds were evaluated for

their anti-proliferative activity against PC-3 cells using an MTT assay. PC-3 cells were seeded in a 96-well plate and cultured for 10 hours at 37 °C. Thereafter, cells were treated with tested compounds at serial concentrations and DMSO (control), and incubate for 72 hours. MTT (5 mg/mL, 10 μ L) was added to the culture and incubated for another 4 hours. Subsequently, the formazan crystal was extracted with DMSO and the absorbance (OD₅₇₀) was detected with a microplate reader (Bio-Rad 680, USA). The IC₅₀ values was calculated with GraphPad Prism (version 5.0).

4.4. Kinase selectivity assay

Compounds are prepared to 50 \times final assay concentration in 100% DMSO, and the working stock of compound is added to the assay well as the first component in the reaction, followed by the remaining components. Kinases are diluted in specific buffer prior to addition to the reaction mix. There is no pre-incubation step between the compound and the kinase prior to initiation of the reaction. The reaction is initiated by the addition of the Mg/ATP mix. After incubation for 40 minutes at room temperature, the reaction is stopped by the addition of phosphoric acid to a concentration of 0.5%. 10 μ L of the reaction is then spotted onto a P30 filtermat and washed four times for 4 minutes in 0.425% phosphoric acid and once in methanol prior to drying and scintillation counting.

The positive control wells contain all components of the reaction, except the compound of interest, and DMSO (at a final concentration of 2%) is included in these wells to control for solvent effects. The blank wells contain all components of the reaction, with a reference inhibitor replacing the compound of interest. This abolishes kinase activity and establishes the base-line (0% kinase activity remaining).

4.5. Western blotting

Western blot analysis was carried out using a whole-cell lysate. PC-3 cells were treated with DMSO, **10h** (1, 5 and 10 μ M) or **GSK690693** (1, 5 and 10 μ M) for 4 hours, respectively. Afterward, the cells were rinsed twice with ice-cold PBS and lysed in a cell lysis buffer (50 mM Tris-HCl, pH 8.0; 1% Nonidet P-40; 0.5% sodium deoxycholate; 0.1% SDS; 150 mM NaCl; 1 mM PMSF; and a protease inhibitor cocktail). Protein concentration of each sample was measured by using bicinchoninic

acid (BCA) protein assay reagent (Thermo Pierce, IL). 20 ug of lysate was loaded into each lane. Antibodies for GSK3 β and AKT (1:1000) were purchased from Santa (Santa Cruz, USA). The secondary antibodies were horseradish peroxidase (HRP)-linked goat-anti rabbit IgG (Santa Cruz, USA). After SDS-PAGE, proteins were electroblotted onto a PVDF membrane. The blots were blocked with 5% BSA/TBST for 1 hour at room temperature, probed with specific ABS overnight at 4°C, washed, incubated with linked goat-anti rabbit IgG (Santa Cruz, USA), and probed with ECL-plus (GE Healthcare, Sweden). The immunoreactive bands were detected using an image analyzer (LAS1000; Fuji Photo Film, Japan).

4.6. Cell apoptosis assay

Apoptosis was quantified by annexin V-FITC/propidium iodide (PI)-binding assay. Cells were seeded in a 6-well plate with 1 μ M, 5 μ M or 10 μ M of **10h** for 48 hours. Treated cells were washed twice with cold phosphate-buffered saline (PBS) and re-suspended in binding buffer (100 μ L), to which 2 μ L of annexin V-FITC and 5 μ L of PI were added. The samples were gently vortexed and incubated for 15 minutes at room temperature in the dark. After addition of 200 μ L of binding buffer, samples were immediately analyzed by flow cytometry using a FACScan flow cytometer (Becton Dickinson, CA). The percentage of apoptotic cells was analysed using a Flowjo software.

4.7. Human liver microsomes metabolic stability assay

Testosterone, diclofenac and propafenone were tested as control drugs in this assay as all of them were substrates of cytochrome P450 enzymes. A DMSO solution of the tested compound (10 mM, 10 μ L/well) and solution of microsome (80 μ L/well) were added to a 96 well plate, this mixture was first incubated at 37°C for 10 min. Then potassium phosphate buffer (100 mM, 10 μ L/well) was added and No Co-Factor (NCF) remaining was evaluated after a further incubation of 60 min. After this pre-warming process, NADPH regenerating system (10 μ L/well) was added and remaining of each compound was tested at 5 time points (5 min, 10 min, 20 min, 30 min and 60 min). At each time point, stop solution (Including 100 ng/ml Tolbutamide

and 100 ng/ml Labetalol, cold in 4°C, 300 µl/well) was added to terminate the reaction. The sampling plates were shaken for approximate 10 min, and then samples were centrifuged at 4000 rpm for 20 min under 4°C to afford the supernatant (100 µl) for LC/MS test. Intrinsic clearance (CL_{int}) and half-life ($T_{1/2}$) values were then calculated. $CL_{int(mic)} = 0.693/\text{half-life}/\text{mg microsome protein per ml}$. $CL_{int(liver)} = CL_{int(mic)} \times (45 \text{ mg microsomal protein/g liver weight}) \times (20 \text{ g liver weight/kg body weight})$.

Conflict of interest

The authors declare no conflict of interest.

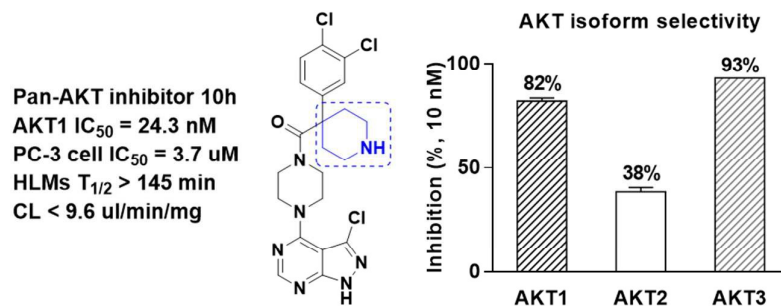
Acknowledgement

This research is funded by Key research and development project of Shandong Province (No. 2017CXGC1401).

References

1. D. A. Altomare and J. R. Testa, *Oncogene*, 2005, **24**, 7455-7464.
2. B. D. Manning and A. Toker, *Cell*, 2017, **169**, 381-405.
3. D. A. Cross, D. R. Alessi, P. Cohen, M. Andjelkovich and B. A. Hemmings, *Nature*, 1995, **378**, 785-789.
4. R. Ferraldeschi, D. Nava Rodrigues, R. Riisnaes, S. Miranda, I. Figueiredo, P. Rescigno, P. Ravi, C. Pezaro, A. Omlin, D. Lorente, Z. Zafeiriou, J. Mateo, A. Altavilla, S. Sideris, D. Bianchini, E. Grist, K. Thway, R. Perez Lopez, N. Tunariu, C. Parker, D. Dearnaley, A. Reid, G. Attard and J. de Bono, *Eur Urol*, 2015, **67**, 795-802.
5. D. A. Heerding, N. Rhodes, J. D. Leber, T. J. Clark, R. M. Keenan, L. V. Lafrance, M. Li, I. G. Safonov, D. T. Takata, J. W. Venslavsky, D. S. Yamashita, A. E. Choudhry, R. A. Copeland, Z. Lai, M. D. Schaber, P. J. Tummino, S. L. Strum, E. R. Wood, D. R. Duckett, D. Eberwein, V. B. Knick, T. J. Lansing, R. T. McConnell, S. Zhang, E. A. Minthorn, N. O. Concha, G. L. Warren and R. Kumar, *J Med Chem*, 2008, **51**, 5663-5679.
6. M. Addie, P. Ballard, D. Buttar, C. Crafter, G. Currie, B. R. Davies, J. Debreczeni, H. Dry, P. Dudley, R. Greenwood, P. D. Johnson, J. G. Kettle, C. Lane, G. Lamont, A. Leach, R. W. Luke, J. Morris, D. Ogilvie, K. Page, M. Pass, S. Pearson and L. Ruston, *J Med Chem*, 2013, **56**, 2059-2073.
7. J. F. Blake, R. Xu, J. R. Bencsik, D. Xiao, N. C. Kallan, S. Schlachter, I. S. Mitchell, K. L. Spencer, A. L. Banka, E. M. Wallace, S. L. Gloor, M. Martinson, R. D. Woessner, G. P. Vigers, B. J. Brandhuber, J. Liang, B. S. Safina, J. Li, B. Zhang, C. Chabot, S. Do, L. Lee, J. Oeh, D. Sampath, B. B. Lee, K. Lin, B. M. Liederer and N. J. Skelton, *J Med Chem*, 2012, **55**, 8110-8127.
8. Y. Liu, Y. Yin, J. Zhang, K. Nomie, L. Zhang, D. Yang, M. L. Wang and G. Zhao, *Arch Pharm*

- (*Weinheim*), 2016, **349**, 356-362.
9. G. Saxty, S. J. Woodhead, V. Berdini, T. G. Davies, M. L. Verdonk, P. G. Wyatt, R. G. Boyle, D. Barford, R. Downham, M. D. Garrett and R. A. Carr, *J Med Chem*, 2007, **50**, 2293-2296.
 10. A. Donald, T. McHardy, M. G. Rowlands, L. J. Hunter, T. G. Davies, V. Berdini, R. G. Boyle, G. W. Aherne, M. D. Garrett and I. Collins, *J Med Chem*, 2007, **50**, 2289-2292.
 11. B. R. Huck and I. Mochalkin, *Bioorg Med Chem Lett*, 2017, **27**, 2838-2848.
 12. T. Liu, W. Zhan, Y. Wang, L. Zhang, B. Yang, X. Dong and Y. Hu, *European journal of medicinal chemistry*, 2014, **73**, 167-176.



Compound 10h is a potent pan-AKT inhibitor showing cellular AKT inhibition and apoptosis induction in PC-3 prostate cancer cells.